J. Sep. Sci. 2008, 31, 548–554

Marta B. Peirotti[1]
Maria V. Piaggio[2]
Julio A. Deiber[1]

[1]Instituto de Desarrollo Tecnológico para la Industria Química (INTEC), Universidad Nacional del Litoral (UNL), Consejo Nacional de Investigaciones Científicas y Técnicas (CONICET), Santa Fe, Argentina
[2]Cátedra de Bioquímica Básica de Macromoléculas, Facultad de Bioquímica y Ciencias Biológicas, UNL, Santa Fe, Argentina

Original Paper

Hydration, charge, size, and shape characteristics of peptides from their CZE analyses

A CZE model is presented for peptide characterization on the basis of well-established physicochemical equations. The effective mobility is used as basic data in the model to estimate relevant peptide properties such as, for instance, hydration, net and total electrical charge numbers, hydrodynamic size and shape, particle average orientation, and pH-microenvironment from the charge regulation phenomenon. Therefore 102 experimental effective mobilities of different peptides are studied and discussed in relation to previous work. An equation for the estimation of peptide hydration as a function of ionizing, polar, and non-polar amino acid residues is included in the model. It is also shown that the shape-orientation factor of peptides may be either lower or higher than one, and its value depends on a complex interplay among total charge number, molar mass, hydration, and amino acid sequence.

Keywords: Hydrodynamic size / Hydration / Net charge number / Peptides / Shape-orientation factor

Received: September 7, 2007; revised: December 3, 2007; accepted: December 6, 2007

DOI 10.1002/jssc.200700426

1 Introduction

CZE is a relevant experimental methodology for the separation and characterization of peptides. This situation is in part justified because high resolution and efficiency, as well as small sample size and short run times, are achieved in modern electrophoresis apparatuses. In this sense, continuous innovations involving both protocol formulations and new experimental setups have been proposed in the literature for improving analyte separation and detection [1–4]. In particular, relevant analyses concerning peptides separations via CZE are now available (see, for instance, [4–9], and citations therein).

In recent years, it has been found that CZE models are becoming important to help in the interpretation of effective mobility data of peptides, from two main points of view [7, 10–22]: (i) effective mobility prediction and optimal protocol formulation in peptide separations; (ii) analysis of experimental effective mobility to characterize peptides from their physicochemical properties, which may be used to study complex biological systems. Indeed, both points of view may be useful for a wide spectrum of applications such as, for instance, identification of peptides fragments from protein digests and characterization of peptides functions as hormones, neurotransmitters, and modern drugs, among many others [23, 24]. In fact, from previous studies, one may conclude that, in applications, at least two types of models for the CZE of peptides are frequently proposed in the literature. One of them consists in predicting the peptide effective mobility (the "direct problem") for a given protocol involving well specified bulk pH, ionic strength I, temperature T, electrical permittivity ε, and viscosity η of the BGE, together with molar mass M (possibly the number of amino acids N) and amino acid sequence (AAS) [9–14, 16–18, 22, 25] or with molecular descriptors [15, 19, 20, 26–28]. The other model (the "inverse problem") involves the peptide characterization, where the effective mobility is provided as basic data and relevant peptide properties are predicted such as, for instance, hydration, electrical net charge, hydrodynamic size and shape, and pH-microenvironment [7, 21, 29, 30]. In the present work we are mainly concerned with the second type of model for the case of CZE of peptides, where 102 experimental effective mobilities of different peptides [14, 15] are reconsidered and discussed in relation to a previous publication [21]. In fact, an equation for the estimation of peptide hydration is now included in the basic model used previously, which was designated as the perturbed Linderstrøm–Lang Capillary Electrophoresis Model (PLLCEM) [21, 31, 32]. In this sense, it should be pointed out that we have considered the characterization of protein, peptides, and amino acids through this model by using effective mobility values of these analytes, avail-

Correspondence: Dr. Julio A. Deiber, INTEC, Güemes 3450, S3000GLN, Santa Fe, Argentina
E-mail: treoflu@ceride.gov.ar
Fax: +54-(0)342-4550944

Abbreviations: AAS, amino acid sequence; **PLLCEM-H**, perturbed Linderstrøm–Lang CZE model

able for a given protocol. Thus, this model was improved in a sequence of studies as a consequence of the analysis of emerging numerical results. In fact, proteins were studied with this model by considering the charge regulation phenomenon [31, 33]. This phenomenon is relevant for the descripti0on of peptide pH-microenvironment from which one estimates the pK shifts of i-ionizing group designated ΔpK_i, the pH near molecule pH^*, and the pH near i-ionizing group indicated as pH_i, for $i = 1 \ldots Nc$. Here Nc is the number of ionizing groups in the analyte, by also accounting for the different positions that each one of them occupies in the macromolecular chain. Then, when peptides were considered [21], we found that for the small ones, rough estimates of hydration designated δ (mass of water per mass of peptide) ought to be included in the model to obtain the appropriate size and shape of the corresponding migrating hydrodynamic particle; otherwise physical inconsistencies like under- and overestimation of hydration could result although the effective mobility value was fitted well. This result was in part a consequence that hydration effects in the modeling became very sensitive to the hydrodynamic particle shape and the orientation of its main axes. Then, for amino acids all these conclusions were corroborated at different pH [32], where it was also appropriate to estimate through an iterative numerical procedure the hydration number $H = \delta M/18$, which is defined as the number of water molecules per analyte chain. In this way the hydration of amino acids was estimated by adding each hydration number value reported in the literature for ionizing h_i^I and polar h_i^{PI}, polar h_i^P, and non-polar h_i^{NP} amino acid residues [32, 34, 35]. Therefore the main purpose of this work is to present the PLLCEM in a reformulated version for peptides, designated here PLLCEM-H, where -H serves to indicate that the hydration number is a result provided by the model solution. Thus Section 2 provides an equation to estimate peptide hydration. Section 3 presents a brief explanation of model equations, some of them already explained in [21, 32], which now includes hydration as well as particle orientation in relation to the direction of the external electrical field E_o, when spheroidal particles are considered. In Section 4, numerical results are presented for different types of peptides (representative cases of the 102 peptides studied here) and they are discussed in relation to previous results to visualize predictions of peptide hydration. Finally, in Section 5, a brief discussion concerning the formulation of CZE models is provided to visualize some needs for further research.

2 Estimation of peptide hydration

For the purposes of this work, peptide hydration is used here to refer to water molecules that on the average migrate with the analyte, without distinction concerning the nature of the bond type [36]. Based on the equivalent spherical particle with an equivalent hydrodynamic radius a_H^e [21], also designated Stokes radius [30], the peptide hydrodynamic volume $V_H = 4\pi a_H^{e\,3}/3$ includes the peptide compact volume $V_c = M v_p/N_A = 4\pi a_c^3/3$ with a compact radius a_c. Here M is the peptide molar mass and v_p is the peptide specific volume calculated through $v_p = \sum_{i=1}^{N} \frac{M_i}{M v_i}$, where v_i is the specific volume [37] and M_i is the molar mass of each amino acid residue composing the peptide AAS. Therefore, the volume $(V_H - V_c)$ is due to hydration, indicating that $a_H^e > a_c$ [21, 38]. In addition, since hydration is the predominant effect increasing V_c to the value V_H, an estimate of δ can be obtained from a numerical knowledge of both a_H^e and a_c (expressed in $\text{Å} = 10^{-10}$ m) through $\delta \approx [(a_H^e/a_c)^3 - 1](v_p/v_w)$ [21, 38] once the model solution provides a_H^e. Also $v_W \approx 1$ cm^3/g is the specific volume of the BGE.

For the calculations carried out in this work, estimations of peptide hydration number H are obtained by summing each hydration number reported in the literature for polar and ionizing, polar and non-polar groups as follows:

$$H \approx h^I_{t-COOH} \left| Z_{COOH} \right| + h^I_{t-NH_3^+} \left| Z_{NH_3^+} \right| + h^{PI}_{t-COOH} (1 - |Z_{t-COOH}|) + h^{PI}_{t-NH_3^+} (1 - |Z_{t-NH_3^+}|) + \sum_{i}^{Nc} \left\{ h_i^I |Z_i| + h_i^{PI}(1 - |Z_i|) + h_i^P + h_i^{NP} \right\} \quad (1)$$

where subscripts t and i refer to terminal groups and side chains of residual amino acids, respectively, composing the peptide. In Eq. (1) values reported by [34] for amino acid residues are used as follows: $h^I_{Asp} = 6$, $h^I_{Glu} = 7.5$, $h^I_{Lys} = 4.5$, $h^I_{Arg} = 3$, $h^I_{His} = 4$, $h^P_{Gly} = 1$, $h^P_{Ser} = 2$, $h^P_{Thr} = 2$, $h^P_{Cys} = 1$, $h^P_{Tyr} = 3$, $h^P_{Asn} = 2$, $h^P_{Gln} = 2$, $h^{NP}_{Ala} = 1.5$, $h^{NP}_{Val} = 1$, $h^{NP}_{Leu} = 1$, $h^{NP}_{Ile} = 1$, $h^{NP}_{Pro} = 3$, $h^{NP}_{Phe} = 0$, $h^{NP}_{Trp} = 2$, $h^{NP}_{Met} = 1$. Other estimations are [32]: $h^I_{t-COOH} \approx 6$, $h^I_{t-NH_3^+} \approx 4.5$, $h^{PI}_{t-COOH} \approx 2$, $h^{PI}_{t-NH_3^+} \approx 2$, $h_i^{PI} \approx 3$.

It is clear that the PLLCEM-H applied to peptides must be consistent with the hydration number estimated from Eq. (1), as described in the following section.

3 PLLCEM–H for peptides

Following previous work [21, 31], the PLLCEM-H considers, in principle, spheroidal particle shapes, including also the spherical one, although it may be extended to other particles shapes. Therefore, the evaluation of peptide net charge requires a knowledge of actual pK_i values of ionizing groups of side chains and ionizing terminal –COOH and $-NH_2$ [21, 31, 32, 39]. pK_i values are mainly

the result of electrostatic interactions among peptide ionizing groups and ions in the BGE, yielding a shift ΔpK_i in the reference pK_i^r reported in [21]. Therefore, the pH-microenvironment around the i-ionizing group defines pH_i, expressed [21, 31, 32] as:

$$pH_i = pH^* + \frac{e^2}{\ln(10)k_BT}\left(\frac{\Delta Z_i}{4\pi r_i^o \varepsilon}\left(\frac{\varepsilon}{\varepsilon'} - 1\right) + \sum_{\substack{j=1 \\ j\neq i}}^{Nc} \frac{\Delta Z_j}{4\pi\varepsilon'} \frac{\exp(-\kappa' r_{ij})}{r_{ij}}\right) \quad (2)$$

In Eq. (2), $\Delta Z_j = Z_j - Z_j^r$ where Z_j^r is the reference charge numbers at site j calculated with pK_j^r, Z_j is the actual charge number at site j, and $r_i^o \approx 1.4$ Å is the effective radius of the i-ionizing group. Also, k_B is the Boltzmann constant and ε' is the electrical permittivity within the peptide domain. Since the inverse of the screening length is $\kappa = \sqrt{2e^2 N_A I 10^3/\varepsilon k_B T}$, where N_A is the Avogadro constant, one obtains $\kappa' = \kappa\sqrt{\varepsilon'/\varepsilon}$. For peptides $\varepsilon' \approx \varepsilon$ [21]. Further $r_{ij} \approx 3.8\sqrt{|i-j|}$ is the approximate generic distance between pairs i–j of ionizing groups in the peptide [21] and pH^* is evaluated by using the mean field approximation expressed [31] as:

$$pH^* = pH + \frac{e^2 Z}{\ln(10)k_BT 4\pi\varepsilon a_H^e(1+\kappa a_H^e)} \quad (3)$$

where Z is the net and Z_T the total peptide charge number, respectively. In order to generate a simple problem, the peptide particle is assumed to have a surface potential provided by Henry's solution [40] and Yoon and Kim's solutions [41] for the effective mobility of spherical and spheroidal particles, respectively [21, 31]. Further, the charge number of i-ionizing group satisfies [32]:

$$Z_i = \pm\frac{1}{1+10^{\mp(pK_i^r - pH_i \pm p\gamma_i)}} \quad (4)$$

where the signs are defined according to basic or acid properties of ionizing groups. In Eq. (4), the activity coefficients γ_i are considered through $p\gamma_i = -\log\gamma_i$ [42, 43] and,

$$p\gamma_i \cong \frac{0.508 Z_i^2\sqrt{I}}{1+\beta\sqrt{I}} \quad (5)$$

where $\beta \approx 1.5$ [44]. In Eqs. (4) and (5), values of Z_i are not known *a priori* as a consequence of the charge regulation phenomenon. They are obtained iteratively through a numerical code [32] modified here in order to introduce Eq. (1). Consequently, the peptide net charge is calculated through

$$eZ = \sum_{i=1}^{Nc} eZ_i \quad (6)$$

Then, to apply the PLLCEM-H with values of peptide effective mobility μ_p, the other relevant equation is,

$$\mu_p = \Omega\mu \quad (7)$$

where

$$\mu = \frac{eZ}{6\pi\eta a_H^e(1+\kappa a_H^e)} f(\kappa a_H^e) \quad (8)$$

is the effective mobility of the equivalent spherical problem, and $f(\kappa a_H^e)$ is Henry's function. Further, the shape-orientation factor Ω may be in particular expressed through the equations providing the effective mobility of spheroidal particles. Therefore, it is readily shown that [21, 41]

$$\Omega = \frac{3}{2} C/f(\kappa a_H^e) \quad (9)$$

where $a_H^e = 2aE_x/\ln\left(\frac{1+E_x}{1-E_x}\right)$ for prolate spheroids, and $a_H^e = aE_x/Cot^{-1}\left(\frac{\sqrt{1-E_x^2}}{E_x}\right)$ for oblate spheroids, both with axes $a > c$ and eccentricity $E_x = \sqrt{1-(c/a)^2}$, when $\kappa a E_x < 1$ and $\frac{aeE_o}{k_BT} < 1$ [21, 32, 40]. Calculations concerning the approximate dimensions a and c of spheroids may be estimated as indicated in [21]. They are not required here for discussing numerical results in Section 4, because any generic hydrodynamic particle is already determined through parameters a_H^e and Ω [32]. This reasoning can be extended to other particle shapes [21], with Ω thus being a quite general hydrodynamic parameter for peptides.

The closure of the PLLCEM-H (Eqs. (2) to (8)) requires the introduction of the hydration number H of the migrating peptide (see Eq. (1)) as relevant property associated with the particle shape. It is also worth mentioning that in order to use Eq. (1) in the computational code described in [21, 32] a new numerical routine has been included which must read from an imputing file, alpha-numeric data introducing the AAS, the amino acids order numbers indicating their positions in the main chain, and hydration numbers of each terminal group and amino acid residues reported in [32, 34, 35]. This numerical routine also includes the calculation of peptide specific volume v_p from the corresponding AAS (see also Table 2).

For calculation purposes, the expressions, $pK_i^r - pH_i \equiv pK_i - pH$ and $\Delta pK_i = pK_i^r - pK_i = pH_i - pH = \Delta pH_i$, are still valid here [31]. Therefore, ΔpK_i of peptide ionizing groups are a direct consequence of pH shifts ΔpH_i, which is the difference between the pH near the ionizing group in the peptide and the pH of the BGE.

Once the values of Ω and a_H^e are known after convergence criteria of the numerical code have been satisfied [32], the resulting hydrodynamic particle shape and orientation may be fixed by considering that in particular spheroidal particles migrate with an average value

$<C> = \alpha C^{//} + C^{\perp}(1-\alpha)$. Coefficients $C^{//}$ and $C^{\perp}$ are provided in [41], where $0 < \alpha < 1$ indicates the degree of the collinear particle orientation defined by its revolution axis with the applied electrical field direction, as described in [21]. Further, when all spheroidal particle orientations are equally probable, one gets $\alpha = 1/3$. Nevertheless, these charged analytes have an electrostatic interaction with E_o having a tendency to bias Brownian motion (see also [38]). This is one of the reasons for obtaining values $\alpha \neq 1/3$ in [21]. For spheroidal particles, the angle θ formed between the spheroidal axis of revolution and the direction of the electrical field E_o may be estimated from α. Therefore, $\alpha = \cos^2\theta$ and $1-\alpha = \sin^2\theta$ on the average, and hence $\theta \approx 55°$ for $\alpha = 1/3$. As a consequence of this result, for $\theta > 55°$ or $\alpha < 1/3$ the mobility tensor component that predominates in the spheroidal migration is $C^{\perp}$. The opposite situation is also true for $\alpha > 1/3$ and $\theta < 55°$.

4 Numerical results and discussion

The PLLCEM-H formulated in Section 2 was used to study the effective mobility of 102 peptides reported in [14, 15] for a running BGE with pH 2.5 and $I = 35.3$ mM at 22°C. In this sense, a relevant result is that the PLLCEM-H provides peptide hydrations within the range $0.27 < \delta < 0.96$ for all the cases studied here, among other peptide properties. Thus this range of values is in good agreement with that expected for peptides and proteins evaluated through other techniques [36, 38]. Further, when the PLLCEM was used in [21] with the nine peptides reported in Table 1 here, out of the 102 studied, the hydration values obtained were rather overestimated because the particle shape was constrained to be spherical ($\Omega = 1$). Now, when the PLLCEM-H is used for the same peptides by allowing also particle shapes different from the spherical one ($\Omega \neq 1$) hydration values are within the physical range placed above, as illustrated in Table 1. These results are important in the sense that the PLLCEM-H is able to provide the peptide hydration number $H = \delta M/18$ through an iterative numerical process that considers the interplay between hydration and shape-orientation factor, equivalent hydrodynamic radius, and net and total charge numbers. The appropriate estimation of hydration is crucial for the modeling of peptide effective mobility because the hydrodynamic friction of the corresponding migrating particle is associated with both peptide molar mass and immobilized water, including water molecules having high residence times around the peptide on the average.

Important numerical results found in general with the 102 peptides studied here, when the spheroidal particle shape is considered, are as follows: (i) The shape-orientation factor is approximately greater than one ($\Omega > 1.05$, with a major tendency to migrate via $C^{//}$ at $\theta < 55°$) for peptides having around $212 < M < 600$ g/mol and $Z_T < 3.5$. These results are validated for 26 peptides with molar masses in this specified range of values. (ii) The shape-orientation factor is approximately less than one ($\Omega < 0.95$, with a major tendency to migrate via $C^{\perp}$ at $\theta > 55°$) for peptides having around $650 < M < 4500$ g/mol. These results are validated for 66 peptides with molar masses in this specified range of values. Furthermore, from numerical results it is observed once more that the shape-orientation factor has a tendency to decrease with high values of Z_T. In this group, a few peptides, coded with numbers 55 and 58 to 64 reported in [21], tend to yield Ω close to or less than 0.5. These particular peptides have a rather high total charge and the Debye–Hückel–Henry hypothesis starts to be a coarse approximations (see also below).

Table 1. Comparison of numerical hydration predictions with the PLLCEM ($\Omega = 1$) and the PLLCEM-H ($\Omega \neq 1$), for typical peptides reported in [21].

AAS	PLLCEM	PLLCEM-H	
	δ	Ω	δ
HMTEVVRHCPHHER	2.17	0.70	0.47
FLTPKKLQCVDLHVISNDV-CAQVHPQKVTK	2.44	0.65	0.39
HQIINMWQEVGKAMYAPPISG-QIRRIHIGPGRAFYTTKN	3.09	0.57	0.35
HMTEVVRRYPHHER	2.05	0.71	0.46
RTHCQSHYRRRHCSR	3.10	0.60	0.45
DRVIEVVQGAYRAIRHIPRRIRQ-GLERRIHIGPGRAFYTTKN	5.59	0.47	0.37
CRHRRRHRRGC	4.08	0.51	0.47
KKKKK	2.62	0.76	0.86
CRHHRRRHRRGC	4.81	0.52	0.47

Table 2 presents typical peptides studied in this work, extracted from the 102 ones, to visualize better through parameters a_H^e, Z, Z_T, pH*, Ω, H, M, and ν_p, the discussion concerning the two peptides groups described in points i and ii above. Further, it is observed that only around 9 peptides, coded with numbers 1, 8, 10, 19, 46, 47 57, 77, and 81 reported in [21], may be considered as spherical particles with around $0.95 < \Omega < 1.05$, having into account that small numerical round off and experimental errors may place them into either groups of points i or ii described above.

Another study carried out in this work was that concerned with the validation of Debye–Hückel–Henry approximations for spheroidal particles, which were introduced through the model formulation. As defined and described previously for spherical particles [31], here the coordinates provided in [45] are used again. Now they are expressed $Y = 3\mu_p e\eta/(2\Omega f(\kappa a_H^e)\varepsilon k_B T)$, $X = e\zeta/(k_B T)$ and $P = \kappa a_H^e$, which are modified to apply them to spher-

Table 2. PLLCEM-H numerical predictions of physicochemical parameters for typical peptides reported in [21], ordered here with increasing molar masses.

AAS	μ_p (10^{-8} $m^2 \cdot V^{-1} \cdot s^{-1}$)	M (g/mol)	Ω	a_H (Å)	Z	Z_T	pH*	H	v_p (cm^3/g)
AAA	1.543	213.30	1.38	5.29	0.89	1.11	2.89	11.44	0.79
FD	1.300	280.20	1.23	5.27	0.84	1.17	2.87	10.09	0.68
YY	1.210	344.40	1.18	5.72	0.90	1.10	2.86	12.91	0.70
ANSK	2.091	418.24	1.11	6.18	1.81	2.19	3.16	17.24	0.69
PARR	2.765	498.24	1.06	6.52	2.71	3.29	3.41	18.18	0.75
HMTE	1.891	515.24	1.06	6.38	1.79	2.21	3.12	17.36	0.67
YGGFL	0.975	555.40	1.07	6.34	0.91	1.09	2.82	12.88	0.75
RPPGF	1.836	572.60	1.06	6.62	1.83	2.17	3.11	17.18	0.74
GIGAVLK	1.550	656.37	0.94	6.93	1.84	2.16	3.07	18.14	0.79
KLVVVGADGV	1.313	956.20	0.94	7.69	1.79	2.21	2.99	23.27	0.76
NSFCMGGMNRR	1.830	1272.50	0.89	8.05	2.79	3.21	3.21	24.33	0.69
VLTTGLPALISW IK	1.050	1508.68	0.85	8.81	1.88	2.12	2.93	30.97	0.78
FIGITEAAANLVPMVATV	0.473	1813.85	0.84	9.18	0.91	1.09	2.69	32.88	0.75
KSSQYIKANSKFIGITE	1.705	1911.81	0.77	9.51	3.73	4.27	3.26	44.61	0.72
VPYEPPEVGSVYHHPLQLHV	1.532	2297.60	0.77	10.15	3.69	4.30	3.19	54.77	0.72
FLTPKKLQCVDLHVISNDV-CAQVHPQKVTK	1.868	3390.10	0.65	11.46	6.25	7.74	3.49	73.54	0.73
HQIINMWQEVGKAMYAPPISG-QIRRIHIGPGRAFYTTKN	1.753	4481.20	0.57	12.43	7.51	8.49	3.55	88.01	0.73

oidal particles, or any generic particle. In fact, coordinate Y is corrected by the factor $\Omega f(\kappa a_H^e)$, to be still able to use the numerical values reported by these authors for the spherical shape. These coordinates indicate the range where Debye–Hückel–Henry approximations apply. Thus peptide experimental value μ_p is introduced into Y, to obtain the corresponding X value, which provides the admissible particle net charge and electrical potential ζ. Within this framework, we found that peptides coded with numbers 55 and 58 to 64 reported in [21] and already considered above, yield rather approximate results due to the high values of total charge number in relation to molar mass. These peptides also have relatively high values of electrical potential and three of them yield too low shape-orientation factors ($\Omega < 0.5$), indicating consistently with the discussion above that the Debye–Hückel–Henry approximations start to be invalid with relatively higher values of coordinate X.

Since CZE is an analytical technique, it is clear that values X, Y, and P calculated with the help of the PLLCEM-H are relevant to visualize the more useful zone of experimentation described by $Y \approx X$, $X < 2.5$, and $P < 3$, thus avoiding undesired complex phenomena of peptide migrations [31, 40, 45]. In fact, for higher values of X and P, significant ion polarization-relaxation may appear. Another relevant consideration is that for low Ω of spheroidal particle shapes [41], additional undesired phenomena in this analytical technique may be found depending on peptide size, by producing non-monotonic effective mobility variations as a function of the product κc. Within this context of analysis, it is clear that the PLLCEM-H allows visualization of the onset of phenomena that may mask the easy interpretation of effective mobility data from CZE.

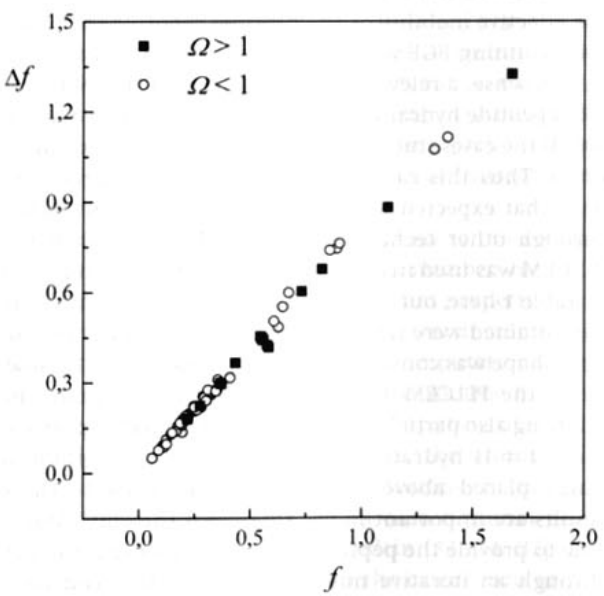

Figure 1. Shape-orientation factor values of 93 peptides having $\Omega \neq 1$, distributed along the near linear relationship between the net $\Delta f = Z/N$ and total $f = Z_T/N$ change number fractions, at pH 2.5.

From the above analysis and the results found in this study, one observes a quite complex interplay among peptide hydration number H, charged numbers Z and Z_T, and shape-orientation factor Ω, which are quantified through the PLLCEM-H. Further, parameter Ω is crucial

to distinguish different peptide hydrodynamic conformations as they are sensed from CZE.

It is also relevant to visualize from Table 2 that values of pH* are greater than the pH of the BGE, consistently with the charge regulation phenomenon described through Eqs. (2) and (3). For the most charged particles, ΔpH_i increases, giving also high ΔpK_i. Thus, the evaluation of pH-microenvironment around the migrating particle is required to quantify the actual peptide net charge.

Finally, it is interesting to show through Fig. 1 that values of the shape-orientation factor of peptides are distributed along the quite linear relationship between the net $\Delta f = Z/N$ and total $f = Z_T/N$ charge number fractions, at pH 2.5. It is observed that peptides with $\Omega < 1$ are placed mainly at relatively low values of Δf and f. Nevertheless, the interplay between charge fractions and shape-orientation of peptides seems to be rather complex.

5 Proposal for further research and concluding remarks

It is not simple to explain definitely why peptides conform to the hydrodynamic shapes described above when spheroidal particles are considered, and when simple considerations of peptide AAS are analyzed. Probably additional information concerning other phenomena such as hydrophobic interactions accounted for through the peptide compact volume must be included. It is also clear that the selection of a type of hydrodynamic shape such as spheroidal particles may still not be enough to represent hydrodynamic particles like those found in actual highly charged complex peptides. The spheroidal particle model is observed to present only two axes of symmetry, and hence the mobility tensor has two components, while in more general cases the three diagonal components of this tensor may be required to represent the actual peptide shape. At present the PLLCEM-H requires the elucidation of a better interpretation of parameter Ω in terms of peptide microstructure, apart from the possibility that more complex shape particle models may be required at this level of detail.

In only few cases can the spherical shape be assumed to be representative of the peptide hydrodynamics. This conclusion, of course, suggests that the particle shapes should not be inputted arbitrarily because the peptide shape must be consistent with numerical estimations of hydration numbers as indicated along this work.

List of symbols

a	major axis of spheroidal particle
a_H^e	equivalent hydrodynamic radius or Stokes radius
a_c	radius of equivalent compact sphere
c	minor axis of spheroidal particle
$C^{//}$	particle mobility parallel to direction of the applied electric field normalized with the asymptotic Smoluchowski mobility
$C^{\perp}$	particle mobility perpendicular to direction of the applied electric field normalized with the asymptotic Smoluchowski mobility
$<C>$	average particle mobility normalized with the asymptotic Smoluchowski mobility
e	elementary charge
E_o	applied electrical field
E_x	spheroidal particle eccentricity
f	total charge fraction of peptide
$f(\kappa a_H^e)$	Henry's function
H	peptide hydration number
h_i	hydration number of amino acid residues. Subscript i indicates amino acid type
h_i^P	hydration number of polar amino acid residues.
h_i^{NP}	hydration number of the non-polar amino acid residues.
h_i^I	hydration number of ionizing amino acid residues
h_i^{PI}	hydration number of ionizing and polar amino acid residues
I	ionic strength
k_B	Boltzmann constant
M	peptide molar mass
M_i	molar mass of i-amino acid residue
N	total number of amino acid residues in peptide
N_c	total number of ionizing groups in peptide
N_A	Avogadro constant
pH	pH of BGE
pH*	pH near molecule
pH_i	microenvironment-pH around the i-ionizing group in peptide
pK_i	actual pK value of i-ionizing group in peptide
pK_i^r	pK value of ionizing groups in the reference state
r_i^o	effective radius of the i-ionizing group in peptide
r_{ij}	generic distance between pairs of i and j ionizing groups in peptide
T	absolute temperature
v_p	peptide specific volume
v_w	BGE specific volume
v_i	specific volume of i-amino acid residue
V_H	peptide hydrodynamic volume
V_c	peptide compact volume
Z	peptide net charge number
Z_i	charge number of i-ionizing group in peptide
Z_i^r	reference charge number of i-ionizing group in peptide
Z_T	peptide total charge number

Δf	net charge fraction of peptide
ΔpH_i	difference between pH_i and pH
ΔpK_i	difference between reference pK_i^r and actual pK_i
ΔZ_j	difference between charge number Z_j and reference charge number Z_j^r
α	degree of collinear particle orientation
δ	peptide hydration
ε	BGE electrical permittivity
ε'	electrical permittivity within the peptide domain
Ω	shape-orientation factor
γ_i	thermodynamic activity coefficient of i-ionizing group in the peptide
κ	inverse of the screening length
κ'	inverse of the screening length within peptide domain
θ	angle between spheroidal axis of revolution and direction of electrical field
η	BGE viscosity
μ	electrophoretic mobility of equivalent spherical particle
μ_p	effective electrophoretic mobility
ζ	particle zeta potential

The authors are grateful for financial aid received from UNL (CAI+D 28157) and CONICET (PIP 05728), Argentina.

6 References

[1] Monton, M. R. N., Terabe, S., *Anal. Sci.* 2005, *21*, 5–13.
[2] Dolnik, V., Liu, S., *J. Sep. Sci.* 2005, *28*, 1994–2009.
[3] Šolínová, V., Kašicka, V., *J. Sep. Sci.* 2006, *29*, 1743–1762.
[4] Kašicka, V., *Electrophoresis* 2006, *27*, 142–175.
[5] Kašicka, V., *Electrophoresis* 1999, *20*, 3084–3105.
[6] Kašicka, V., *Electrophoresis* 2001, *22*, 4139–4162.
[7] Messana, I., Rossetti, D. V., Cassiano, L., Misiti, F., Giardina, B., Castagnola, M., *J. Chromatogr. B* 1997, *699*, 149–171.
[8] Koval, D., Kašicka, V., Jirácek, J., Collinsová, M., *Electrophoresis* 2003, *24*, 774–781.
[9] Šolínová, V., Kašicka, V., Koval, D., Hlavácek, J., *Electrophoresis* 2004, *25*, 2299–2308.
[10] Offord, R. E., *Nature* 1966, *211*, 591–593.
[11] Rickard, E. C., Strohl, M. M., Nielsen, R. G., *Anal. Biochem.* 1991, *197*, 197–207.
[12] Grossman, P. D., Colburn, J. C., Lauer, H. H., *Anal. Biochem.* 1989, *179*, 28–33.
[13] Cifuentes, A., Poppe, H., *Electrophoresis* 1995, *16*, 516–524.
[14] Janini, G. M., Metral, C. J., Isaaq, H. J., Muschik, G. M., *J. Chromatogr. A* 1999, *848*, 417–433.
[15] Janini, G. M., Metral, C. J., Isaaq, H. J., *J. Chromatogr. A* 2001, *924*, 291–306.
[16] Cross, R. F., Cao, J., *J. Chromatogr. A* 1997, *786*, 171–180.
[17] Cross, R. F., Wong, M. G., *Chromatographia* 2001, *53*, 431–436.
[18] Cross, R. F., Garnham, N. F., *Chromatographia* 2001, *54*, 639–646.
[19] Jalali-Heravi, M., Shen, Y., Hassanisadi, M., Khaledi, M. G., *J. Chromatogr. A* 2005, *1096*, 58–68.
[20] Jalali-Heravi, M., Shen, Y., Hassanisadi, M., Khaledi, M. G., *Electrophoresis* 2005, *26*, 1874–1885.
[21] Piaggio, M. V., Peirotti, M. B., Deiber, J. A., *Electrophoresis* 2006, *27*, 4631–4647.
[22] Xin, Y., Mitchell, H., Cameron, H., Allison, S. A., *J. Phys. Chem. B* 2006, *110*, 1038–1045.
[23] Simó, C., González, R., Barbas, C., Cifuentes, A., *Anal. Chem.* 2005, *77*, 7709–7716.
[24] Benavente, F., Balaguer, E., Barbosa, J., Sanz-Nebot, V., *J. Chromatogr. A* 2006, *1117*, 94–102.
[25] Castagnola, M., Rossetti, D. V., Corda, M., Pellegrini, M., Misiti, F., Olianas, A., Giardina, B., Messana, I., *Electrophoresis* 1998, *19*, 2273–2277.
[26] Liu, H. X., Yao, X. J., Xue, C. X., Zhang, R. S., Liu, M. C., Hu, Z. D., Fan, B. T., *Anal. Chim. Acta* 2005, *542*, 249–259.
[27] Ma, W., Luan, F., Zhang, H., Zhang, X., Liu, M., Hu, Z., Fan, B., *Analyst* 2006, *131*, 1254–1260.
[28] Yu, K., Cheng, Y., *Talanta* 2007, *71*, 676–682.
[29] Hearn, M. T. W., Keah, H. H., Boysen, R. I., Messana, I., Misiti, F., Rossetti, D. V., Giardina, B., Castagnola, M., *Anal. Chem.* 2000, *72*, 1964–1972.
[30] Castagnola, M., Rossetti, D. V., Cassiano, L., Misiti, F., Pennacchietti, L., Giardina, B., Messana, I., *Electrophoresis* 1996, *17*, 1925–1930.
[31] Piaggio, M. V., Peirotti, M. B., Deiber, J. A., *Electrophoresis* 2005, *26*, 3232–3246.
[32] Piaggio, M. V., Peirotti, M. B., Deiber, J. A., *Electrophoresis* 2007, *28*, 3658–3673.
[33] Linderstrøm-Lang, K. C., *Trav. Lab. Carlsberg* 1924, *15*, 1–29.
[34] Kuntz, I. D., *J. Am. Chem. Soc.* 1971, *93*, 514–516.
[35] Kuntz, I. D., *J. Am. Chem. Soc.* 1971, *93*, 516–518.
[36] Fennema, O. in: Whitaker J. R., Tannenbaum, S. R. (Eds.), *Food Proteins*, AVI Publishing Co., Inc., Connecticut, 1977, pp. 50–90.
[37] Creighton, T. E., *Proteins: Structures and Molecular Properties*, W. H. Freeman and Company, New York 1993.
[38] Tanford, Ch., *Physical Chemistry of Macromolecules*, John Wiley & Sons, New York 1961, pp. 457–488.
[39] Antosiewicz, J., McCammnon, J. A., Gilson, M. K., *Biochemistry* 1996, *35*, 7819–7833.
[40] Russell, W. B., Saville, D. A., Schowalter, W. R., *Colloidal Dispersions*, Cambridge University Press, Cambridge, UK 1989, pp. 96–108.
[41] Yoon, B. J., Kim, S., *J. Colloid Interface Sci.* 1989, *128*, 275–288.
[42] Survay, M. A., Goodall, D. M., Wren, S. A. C., Rowe, R. C., *J. Chromatogr. A* 1996, *741*, 99–113.
[43] Vcelaková, K., Zusková, I., Kenndler, E., Gaš, B., *Electrophoresis* 2004, *25*, 309–317.
[44] Koval, D., Kašicka, V., Zusková, I., *Electrophoresis* 2005, *26*, 3221–3231.
[45] O'Brien, R. W., White, L. R., *J. Chem. Soc. Faraday Trans.* 1978, *74*, 1607–1626.

